

The latter events can be observed only indirectly because neither the K_2^0 nor the neutron is seen. Figure 2(c) shows the "missing mass" spectrum for events which have a K_1^0 as the only visible collision product. The events in the KN region of phase space must be corrected for contamination from $K_1^0 K_1^0 n$, $\pi^0 K^0 \Lambda^0$, $\pi^0 K^0 \Sigma^0$ final states. This was easily done at 1.89 BeV/c since all these reactions have been studied in a previous experiment at that momentum.⁹ The result shows there were $(17 \pm 8) K_1^0 K_2^0 n$ events and $(15 \pm 7) K^- K^0 p$ events, which compares favorably with the equal number called for by the one-pion-exchange model.

Provided the one-pion-exchange model is valid, one may place rather strict limits on the angular momentum of the $K\bar{K}$ system. Since the G parity of the $\pi\pi$ system is even, we have¹⁰ $G = (-1)^{L+I} = +1$, where L is the angular momentum of the $K\bar{K}$ system and I is the isotopic spin. The data in Fig. 2(a) then suggest the low-energy cross section for $\pi\pi \rightarrow K\bar{K}$ is ~ 2 mb for $I=0$, $L=0$ K pairs and ~ 0.6 mb for $I=1$, $L=1$ K pairs. Both cross sections drop to low values for energies of 100 MeV or more above threshold for the $K\bar{K}$ system.

Eight examples of K^+K^- production [reaction (3)] observed in this experiment were not included in the foregoing analysis. The signature of these events is a charged K^+ decay, which is sensitive to the K momentum spectrum. Additional bias may result from the difficulty in distinguishing some of these events from Σ^+ decays. In our

sample of eight events the K^+K^- masses occur in the lower half of phase space in a manner similar to reaction (1), but the recoil nucleon tends to go forward. This latter observation may indicate that not all K pairs are produced in peripheral collisions.

We would like to thank Dr. R. G. Sachs, Dr. C. Goebel, and Dr. Marc Ross for helpful discussions concerning this data. We are grateful to J. Boyd and S. S. Lee for their help with calculations and preparation of the data.

*Work supported in part by the U. S. Atomic Energy Commission and the Wisconsin Alumni Research Foundation.

¹M. Baker and F. Zachariasen, Phys. Rev. **119**, 438 (1960).

²Mao-Chen, Phys. Rev. **125**, 2125 (1962).

³G. Costa and L. Tenaglia (to be published).

⁴Proceedings of the Aix-en-Provence Conference on Elementary Particles, 1961 (C.E.N. Saclay, France, 1961), Vol. 1, p. 101.

⁵G. F. Chew and F. E. Low, Phys. Rev. **113**, 1640 (1959).

⁶F. Salzman and G. Salzman, Phys. Rev. **120**, 599 (1960).

⁷A. R. Erwin, R. H. March, W. D. Walker, and E. West, Phys. Rev. Letters **6**, 628 (1961).

⁸M. Goldhaber, T. D. Lee, and C. N. Yang, Phys. Rev. **112**, 1796 (1958).

⁹A. R. Erwin, R. H. March, and W. D. Walker, Nuovo cimento **24**, 237 (1962).

¹⁰We have assumed throughout that the intrinsic $K\bar{K}$ parity product is even.

OBSERVATION OF HIGH-ENERGY NEUTRINO REACTIONS AND THE EXISTENCE OF TWO KINDS OF NEUTRINOS*

G. Danby, J.-M. Gaillard, K. Goulianos, L. M. Lederman, N. Mistry,
M. Schwartz,[†] and J. Steinberger[†]

Columbia University, New York, New York and Brookhaven National Laboratory, Upton, New York
(Received June 15, 1962)

In the course of an experiment at the Brookhaven AGS, we have observed the interaction of high-energy neutrinos with matter. These neutrinos were produced primarily as the result of the decay of the pion:

$$\pi^\pm \rightarrow \mu^\pm + (\nu/\bar{\nu}). \quad (1)$$

It is the purpose of this Letter to report some of the results of this experiment including (1) demonstration that the neutrinos we have used pro-

duce μ mesons but do not produce electrons, and hence are very likely different from the neutrinos involved in β decay and (2) approximate cross sections.

Behavior of cross section as a function of energy. The Fermi theory of weak interactions which works well at low energies implies a cross section for weak interactions which increases as phase space. Calculation indicates that weak interacting cross sections should be in the neigh-

borhood of 10^{-38} cm² at about 1 BeV. Lee and Yang¹ first calculated the detailed cross sections for

$$\begin{aligned} \nu+n &\rightarrow p+e^-, \\ \bar{\nu}+p &\rightarrow n+e^+, \end{aligned} \quad (2)$$

$$\begin{aligned} \nu+n &\rightarrow p+\mu^-, \\ \bar{\nu}+p &\rightarrow n+\mu^+, \end{aligned} \quad (3)$$

using the vector form factor deduced from electron scattering results and assuming the axial vector form factor to be the same as the vector form factor. Subsequent work has been done by Yamaguchi² and Cabbibo and Gatto.³ These calculations have been used as standards for comparison with experiments.

Unitarity and the absence of the decay $\mu \rightarrow e + \gamma$. A major difficulty of the Fermi theory at high energies is the necessity that it break down before the cross section reaches $\pi\lambda^2$, violating unitarity. This breakdown must occur below 300 BeV in the center of mass. This difficulty may be avoided if an intermediate boson mediates the weak interactions. Feinberg⁴ pointed out, however, that such a boson implies a branching ratio $(\mu \rightarrow e + \gamma)/(\mu \rightarrow e + \nu + \bar{\nu})$ of the order of 10^{-4} , unless the neutrinos associated with muons are different from those associated with electrons.⁵ Lee and Yang⁶ have subsequently noted that any general mechanism which would preserve unitarity should lead to a $\mu \rightarrow e + \gamma$ branching ratio not too different from the above. Inasmuch as the branching ratio is measured to be $\leq 10^{-8}$,⁷ the hypothesis that the two neutrinos may

be different has found some favor. It is expected that if there is only one type of neutrino, then neutrino interactions should produce muons and electrons in equal abundance. In the event that there are two neutrinos, there is no reason to expect any electrons at all.

The feasibility of doing neutrino experiments at accelerators was proposed independently by Pontecorvo⁸ and Schwartz.⁹ It was shown that the fluxes of neutrinos available from accelerators should produce of the order of several events per day per 10 tons of detector.

The essential scheme of the experiment is as follows: A neutrino "beam" is generated by decay in flight of pions according to reaction (1). The pions are produced by 15-BeV protons striking a beryllium target at one end of a 10-ft long straight section. The resulting entire flux of particles moving in the general direction of the detector strikes a 13.5-m thick iron shield wall at a distance of 21 m from the target. Neutrino interactions are observed in a 10-ton aluminum spark chamber located behind this shield.

The line of flight of the beam from target to detector makes an angle of 7.5° with respect to the internal proton direction (see Fig. 1). The operating energy of 15 BeV is chosen to keep the muons penetrating the shield to a tolerable level.

The number and energy spectrum of neutrinos from reaction (1) can be rather well calculated, on the basis of measured pion-production rates¹⁰ and the geometry. The expected neutrino flux from π decay is shown in Fig. 2. Also shown is

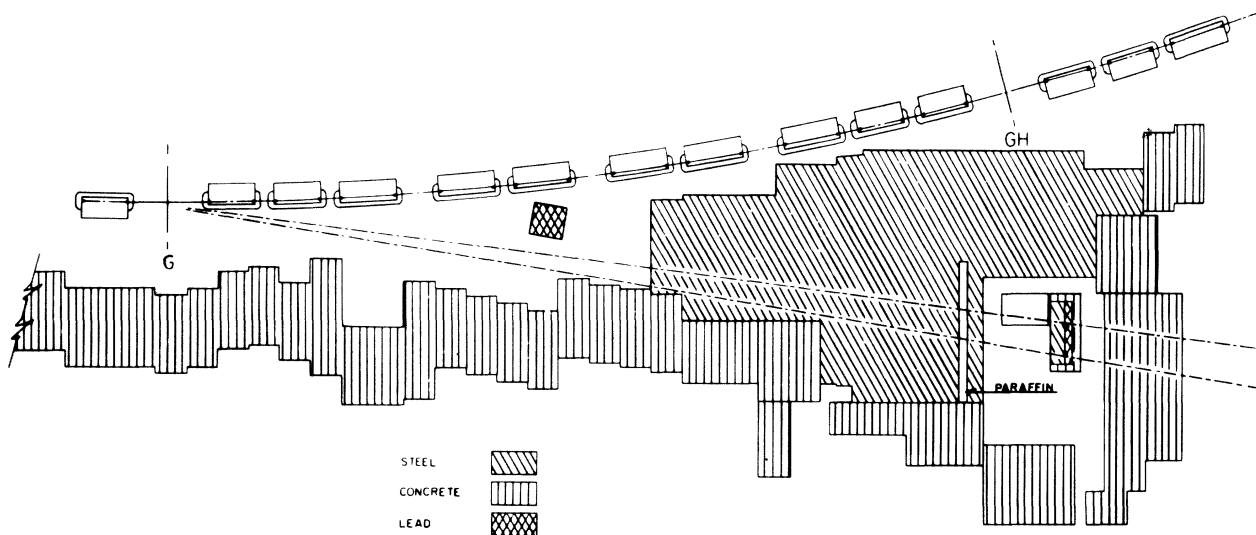


FIG. 1. Plan view of AGS neutrino experiment.

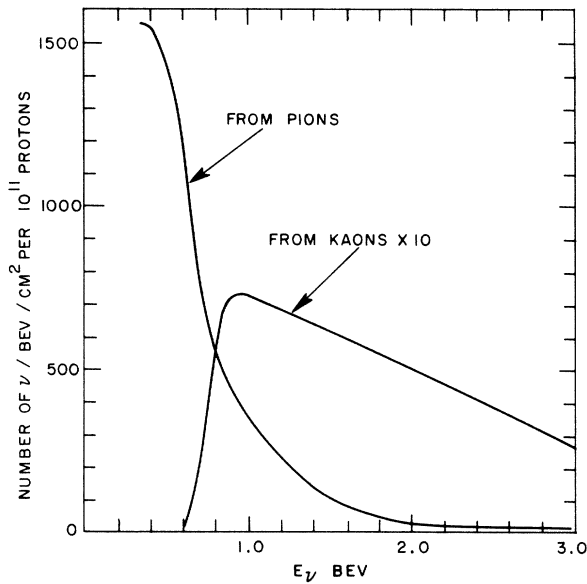


FIG. 2. Energy spectrum of neutrinos expected in the arrangement of Fig. 1 for 15-BeV protons on Be.

an estimate of neutrinos from the decay $K^{\pm} \rightarrow \mu^{\pm} + \nu(\bar{\nu})$. Various checks were performed to compare the targeting efficiency (fraction of circulating beam that interacts in the target) during the neutrino run with the efficiency during the beam survey run. (We believe this efficiency to be close to 70%.) The pion-neutrino flux is considered reliable to approximately 30% down to 300 MeV/c, but the flux below this momentum does not contribute to the results we wish to present.

The main shielding wall thickness, 13.5 m for most of the run, absorbs strongly interacting particles by nuclear interaction and muons up to 17 BeV by ionization loss. The absorption mean free path in iron for pions of 3, 6, and 9 BeV has been measured to be less than 0.24 m.¹¹ Thus the shield provides an attenuation of the order of 10^{-24} for strongly interacting particles. This attenuation is more than sufficient to reduce these particles to a level compatible with this experiment. The background of strongly interacting particles within the detector shield probably enters through the concrete floor and roof of the 5.5-m thick side wall. Indications of such leaks were, in fact, obtained during the early phases of the experiment and the shielding subsequently improved. The argument that our observations are not induced by strongly interacting particles will also be made on the basis of the detailed structure of the data.

The spark chamber detector consists of an array of 10 one-ton modules. Each unit has 9 aluminum plates 44 in. \times 44 in. \times 1 in. thick, separated by $\frac{3}{8}$ -in. Lucite spacers. Each module is driven by a specially designed high-pressure spark gap and the entire assembly triggered as described below. The chamber will be more fully described elsewhere. Figure 3 illustrates the arrangement of coincidence and anticoincidence counters. Top, back, and front anticoincidence sheets (a total of 50 counters, each 48 in. \times 11 in. \times $\frac{1}{2}$ in.) are provided to reduce the effect of cosmic rays and AGS-produced muons which penetrate the shield. The top slab is shielded against neutrino events by 6 in. of steel and the back slab by 3 ft of steel and lead.

Triggering counters were inserted between adjacent chambers and at the end (see Fig. 3). These consist of pairs of counters, 48 in. \times 11 in. \times $\frac{1}{2}$ in., separated by $\frac{3}{4}$ in. of aluminum, and in fast coincidence. Four such pairs cover a chamber; 40 are employed in all.

The AGS at 15 BeV operates with a repetition period of 1.2 sec. A rapid beam deflector drives the protons onto the 3-in. thick Be target over a period of 20-30 μ sec. The radiation during this interval has rf structure, the individual bursts being 20 nsec wide, the separation 220 nsec. This structure is employed to reduce the total "on" time and thus minimize cosmic-ray background. A Čerenkov counter exposed

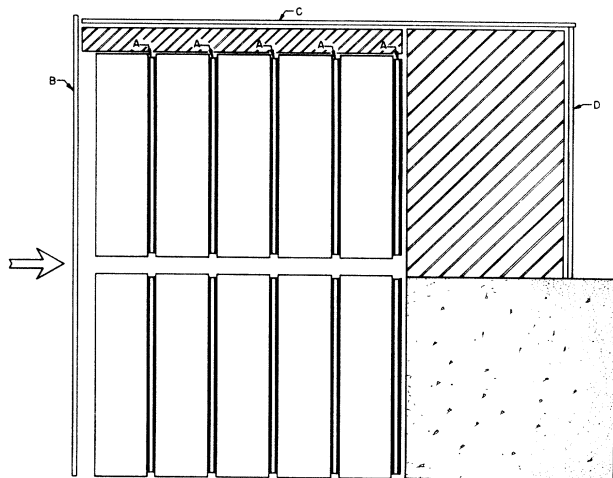


FIG. 3. Spark chamber and counter arrangement. A are the triggering slabs; B, C, and D are anticoincidence slabs. This is the front view seen by the four-camera stereo system.

to the pions in the neutrino "beam" provides a train of 30-nsec gates, which is placed in coincidence with the triggering events. The correct phasing is verified by raising the machine energy to 25 BeV and counting the high-energy muons which now penetrate the shield. The tight timing also serves the useful function of reducing sensitivity to low-energy neutrons which diffuse into the detector room. The trigger consists of a fast twofold coincidence in any of the 40 coincidence pairs in anticoincidence with the anticoincidence shield. Typical operation yields about 10 triggers per hour. Half the photographs are blank, the remainder consist of AGS muons entering unprotected faces of the chamber, cosmic rays, and "events." In order to verify the operation of circuits and the gap efficiency of the chamber, cosmic-ray test runs are conducted every four hours. These consist of triggering on almost horizontal cosmic-ray muons and recording the results both on film and on Land prints for rapid inspection (see Fig. 4).

A convenient monitor for this experiment is the number of circulating protons in the AGS machine. Typically, the AGS operates at a level of $2-4 \times 10^{11}$ protons per pulse, and 3000 pulses per hour. In an exposure of 3.48×10^{17} protons, we have counted 113 events satisfying the following geometric criteria: The event originates within a fiducial volume whose boundaries lie 4 in. from the front and back walls of the chamber and 2 in. from the top and bottom walls. The first two gaps must not fire, in order to exclude events whose origins lie outside the chambers. In addition, in the case of events consisting of a single track, an extrapolation of the track backwards (towards the neutrino source) for two gaps must also remain within the fiducial volume. The production angle of these single tracks relative to the neutrino line of flight must be less than 60° .

These 113 events may be classified further as follows:

(a) 49 short single tracks. These are single

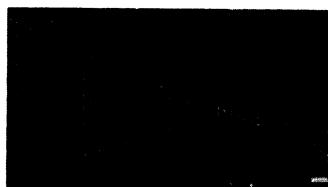


FIG. 4. Land print of Cosmic-ray muons integrated over many incoming tracks.

tracks whose visible momentum, if interpreted as muons, is less than 300 MeV/c. These presumably include some energetic muons which leave the chamber. They also include low-energy neutrino events and the bulk of the neutron produced background. Of these, 19 have 4 sparks or less. The second half of the run (1.7×10^{17} protons) with improved shielding yielded only three tracks in this category. We will not consider these as acceptable "events."

(b) 34 "single muons" of more than 300 MeV/c. These include tracks which, if interpreted as muons, have a visible range in the chambers such that their momentum is at least 300 MeV/c. The origin of these events must not be accompanied by more than two extraneous sparks. The latter requirement means that we include among "single tracks" events showing a small recoil. The 34 events are tabulated as a function of momentum in Table I. Figure 5 illustrates 3 "single muon" events.

(c) 22 "vertex" events. A vertex event is one whose origin is characterized by more than one track. All of these events show a substantial energy release. Figure 6 illustrates some of these.

(d) 8 "showers." These are all the remaining events. They are in general single tracks, too irregular in structure to be typical of μ mesons, and more typical of electron or photon showers. From these 8 "showers," for purposes of comparison with (b), we may select a group of 6 which are so located that their potential range within the chamber corresponds to μ mesons in excess of 300 MeV/c.

In the following, only the 56 energetic events of type (b) (long μ 's) and type (c) (vertex events) will be referred to as "events."

Arguments on the neutrino origin of the ob-

Table I. Classification of "events."

Single tracks			
$p_\mu < 300$ MeV/c ^a	49	$p_\mu > 500$	8
$p_\mu > 300$	34	$p_\mu > 600$	3
$p_\mu > 400$	19	$p_\mu > 700$	2
Total "events" 34			
Vertex events			
Visible energy released < 1 BeV		15	
Visible energy released > 1 BeV		7	

^aThese are not included in the "event" count (see text).

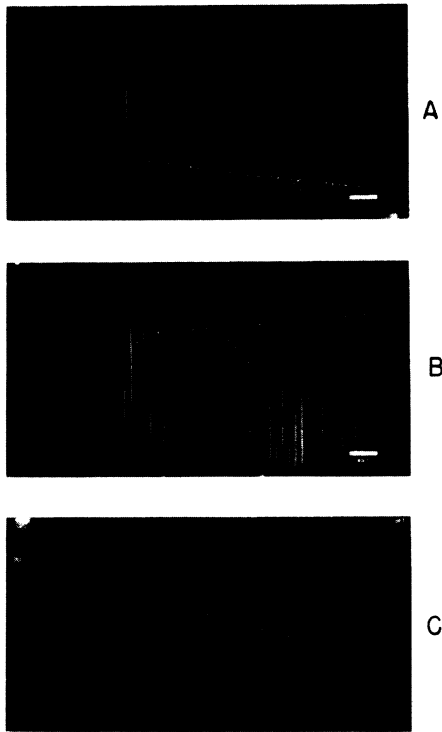


FIG. 5. Single muon events. (A) $p_\mu > 540$ MeV and δ ray indicating direction of motion (neutrino beam incident from left); (B) $p_\mu > 700$ MeV/c; (C) $p_\mu > 440$ with δ ray.

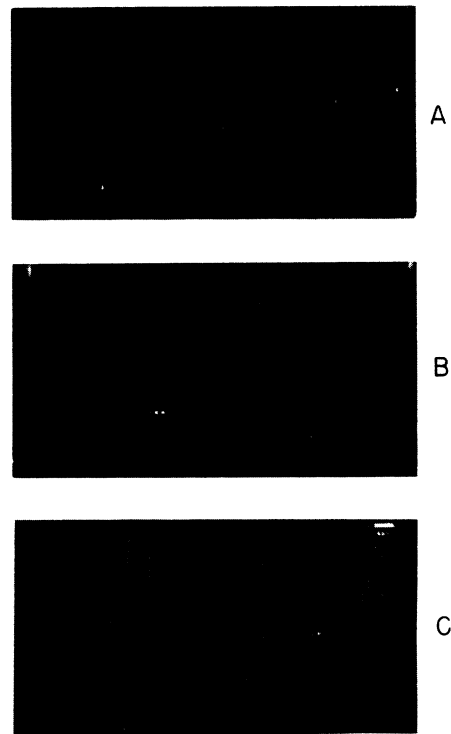


FIG. 6. Vertex events. (A) Single muon of $p_\mu > 500$ MeV and electron-type track; (B) possible example of two muons, both leave chamber; (C) four prong star with one long track of $p_\mu > 600$ MeV/c.

served "events."

1. The "events" are not produced by cosmic rays. Muons from cosmic rays which stop in the chamber can and do simulate neutrino events. This background is measured experimentally by running with the AGS machine off on the same triggering arrangement except for the Čerenkov gating requirement. The actual triggering rate then rises from 10 per hour to 80 per second (a dead-time circuit prevents jamming of the spark chamber). In 1800 cosmic-ray photographs thus obtained, 21 would be accepted as neutrino events. Thus 1 in 90 cosmic-ray events is neutrino-like. Čerenkov gating and the short AGS pulse effect a reduction by a factor of $\sim 10^{-6}$ since the circuits are "on" for only $3.5 \mu\text{sec}$ per pulse. In fact, for the body of data represented by Table I, a total of 1.6×10^6 pulses were counted. The equipment was therefore sensitive for a total time of 5.5 sec. This should lead to $5.5 \times 80 = 440$ cosmic-ray tracks which is consistent with observation. Among these, there should be 5 ± 1 cosmic-ray induced "events." These are almost evident in the small asym-

metry seen in the angular distributions of Fig.

7. The remaining 51 events cannot be the result of cosmic rays.

2. The "events" are not neutron produced. Several observations contribute to this conclusion.

(a) The origins of all the observed events are uniformly distributed over the fiducial volume, with the obvious bias against the last chamber induced by the $p_\mu > 300$ MeV/c requirement. Thus there is no evidence for attenuation, although the mean free path for nuclear interaction in aluminum is 40 cm and for electromagnetic interaction 9 cm.

(b) The front iron shield is so thick that we can expect less than 10^{-4} neutron induced reactions in the entire run from neutrons which have penetrated this shield. This was checked by removing 4 ft of iron from the front of the thick shield. If our events were due to neutrons in line with the target, the event rate would have increased by a factor of one hundred. No such effect was observed (see Table II). If neutrons penetrate the shield, it must be from other di-

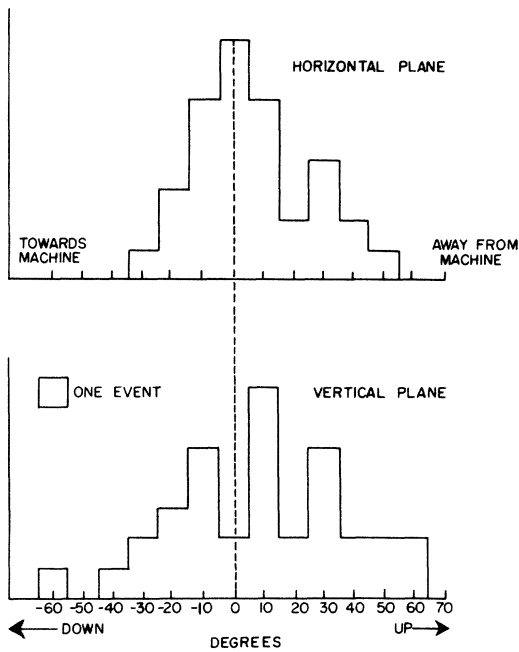


FIG. 7. Projected angular distributions of single track events. Zero degree is defined as the neutrino direction.

reactions. The secondaries would reflect this directionality. The observed angular distribution of single track events is shown in Fig. 7. Except for the small cosmic-ray contribution to the vertical plane projection, both projections are peaked about the line of flight to the target. (c) If our 29 single track events (excluding cosmic-ray background) were pions produced by neutrons, we would have expected, on the basis of known production cross sections, of the order of 15 single π^0 's to have been produced. No cases of unaccompanied π^0 's have been observed.

Table II. Event rates for normal and background conditions.

	Circulating protons $\times 10^{16}$	No. of Events	Calculated cosmic-ray ^c contribution	Net rate per 10^{16}
Normal run	34.8	56	5	1.46
Background I ^a	3.0	2	0.5	0.5
Background II ^b	8.6	4	1.5	0.3

^a 4 ft of Fe removed from main shielding wall.

^b As above, but 4 ft of Pb placed within 6 ft of Be target and subtending a horizontal angular interval from 4° to 11° with respect to the internal proton beam.

^c These should be subtracted from the "single muon" category.

3. The single particles produced show little or no nuclear interaction and are therefore presumed to be muons. For the purpose of this argument, it is convenient to first discuss the second half of our data, obtained after some shielding improvements were effected. A total traversal of 820 cm of aluminum by single tracks was observed, but no "clear" case of nuclear interaction such as large angle or charge exchange scattering was seen. In a spark chamber calibration experiment at the Cosmotron, it was found that for 400-MeV pions the mean free path for "clear" nuclear interactions in the chamber (as distinguished from stoppings) is no more than 100 cm of aluminum. We should, therefore, have observed of the order of 8 "clear" interactions; instead we observed none. The mean free path for the observed single tracks is then more than 8 times the nuclear mean free path.

Included in the count are 5 tracks which stop in the chamber. Certainly a fraction of the neutrino secondaries must be expected to be produced with such small momentum that they would stop in the chamber. Thus, none of these stoppings may, in fact, be nuclear interactions. But even if all stopping tracks are considered to represent nuclear interactions, the mean free path of the observed single tracks must be 4 nuclear mean free paths.

The situation in the case of the earlier data is more complicated. We suspect that a fair fraction of the short single tracks then observed are, in fact, protons produced in neutron collisions. However, similar arguments can be made also for these data which convince us that the energetic single track events observed then are also non-interacting.¹²

It is concluded that the observed single track events are muons, as expected from neutrino interactions.

4. The observed reactions are due to the decay products of pions and K mesons. In a second background run, 4 ft of iron were removed from the main shield and replaced by a similar quantity of lead placed as close to the target as feasible. Thus, the detector views the target through the same number of mean free paths of shielding material. However, the path available for pions to decay is reduced by a factor of 8. This is the closest we could come to "turning off" the neutrinos. The results of this run are given in terms of the number of events per 10^{16} circulating protons in Table II. The rate of "events" is reduced from 1.46 ± 0.2 to 0.3 ± 0.2 per 10^{16} in-

cident protons. This reduction is consistent with that which is expected for neutrinos which are the decay products of pions and K mesons.

Are there two kinds of neutrinos? The earlier discussion leads us to ask if the reactions (2) and (3) occur with the same rate. This would be expected if ν_μ , the neutrino coupled to the muon and produced in pion decay, is the same as ν_e , the neutrino coupled to the electron and produced in nuclear beta decay. We discuss only the single track events where the distinction between single muon tracks of $p_\mu > 300$ MeV/c and showers produced by high-energy single electrons is clear. See Figs. 8 and 4 which illustrate this difference.

We have observed 34 single muon events of which 5 are considered to be cosmic-ray background. If $\nu_\mu = \nu_e$, there should be of the order of 29 electron showers with a mean energy greater than 400 MeV/c. Instead, the only candidates which we have for such events are six "showers" of qualitatively different appearance from those of Fig. 8. To argue more precisely, we have exposed two of our one-ton spark chamber modules to electron beams at the Cosmotron. Runs were taken at various electron energies. From these we establish that the triggering efficiency for 400-MeV electrons is 67%. As a quantity characteristic of the calibration showers, we have taken the total number of observed sparks. The mean number is roughly linear with electron energy up to 400 MeV/c. Larger showers saturate the two chambers

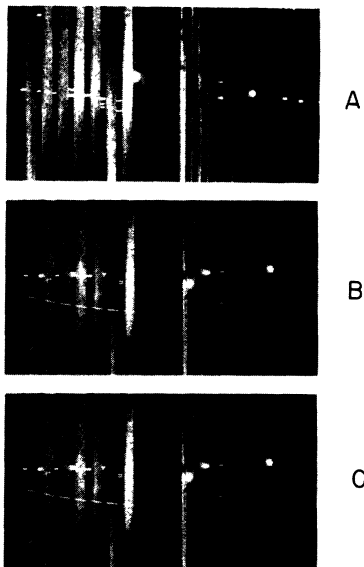


FIG. 8. 400-MeV electrons from the Cosmotron.

which were available. The spark distribution for 400 MeV/c showers is plotted in Fig. 9, normalized to the $\frac{2}{3} \times 29$ expected showers. The six "shower" events are also plotted. It is evident that these are not consistent with the prediction based on a universal theory with $\nu_\mu = \nu_e$. It can perhaps be argued that the absence of electron events could be understood in terms of the coupling of a single neutrino to the electron which is much weaker than that to the muon at higher momentum transfers, although at lower momentum transfers the results of β decay, μ capture, μ decay, and the ratio of $\pi \rightarrow \mu + \nu$ to $\pi \rightarrow e + \nu$ decay show that these couplings are equal.¹³ However, the most plausible explanation for the absence of the electron showers, and the only one which preserves universality, is then that $\nu_\mu \neq \nu_e$; i.e., that there are at least two types of neutrinos. This also resolves the problem raised by the forbiddenness of the $\mu^+ \rightarrow e^+ + \gamma$ decay.

It remains to understand the nature of the 6 "shower" events. All of these events were obtained in the first part of the run during conditions in which there was certainly some neutron background. It is not unlikely that some of the events are small neutron produced stars. One or two could, in fact, be μ mesons. It should also be remarked that of the order of one or two electron events are expected from the neutrinos produced in the decays $K^+ \rightarrow e^+ + \nu_e + \pi^0$ and

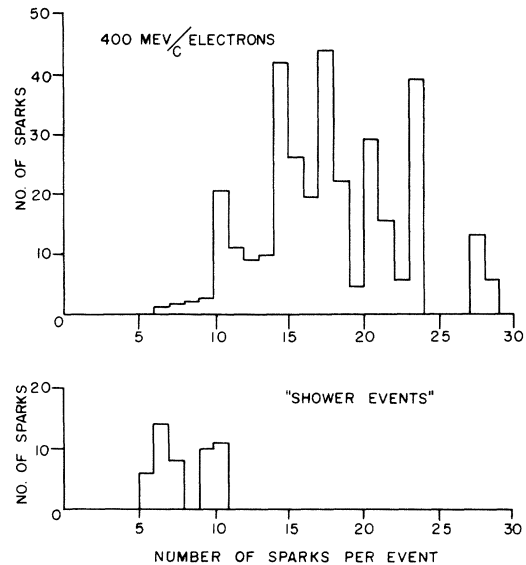


FIG. 9. Spark distribution for 400-MeV/c electrons normalized to expected number of showers. Also shown are the "shower" events.

$$K_2^0 \rightarrow e^\pm + \nu_e + \pi^\mp.$$

The intermediate boson. It has been pointed out¹ that high-energy neutrinos should serve as a reasonable method of investigating the existence of an intermediate boson in the weak interactions. In recent years many of the objections to such a particle have been removed by the advent of $V-A$ theory¹⁴ and the remeasurement of the ρ value in μ decay.¹⁵ The remaining difficulty pointed out by Feinberg,⁴ namely the absence of the decay $\mu \rightarrow e + \gamma$, is removed by the results of this experiment. Consequently it is of interest to explore the extent to which our experiment has been sensitive to the production of these bosons.

Our neutrino intensity, in particular that part contributed by the K -meson decays, is sufficient to have produced intermediate bosons if the boson had a mass m_w less than that of the mass of the proton (m_p). In particular, if the boson had a mass equal to $0.6m_p$, we should have produced ~ 20 bosons by the process $\nu + p \rightarrow w^+ + \mu^- + p$. If $m_w = m_p$, then we should have observed 2 such events.¹⁶

Indeed, of our vertex events, 5 are consistent with the production of a boson. Two events, with two outgoing prongs, one of which is shown in Fig. 6(B), are consistent with both prongs being muons. This could correspond to the decay mode $w^+ \rightarrow \mu^+ + \nu$. One event shows four outgoing tracks, each of which leaves the chamber after traveling through 9 in. of aluminum. This might in principle be an example of $w^+ \rightarrow \pi^+ + \pi^- + \pi^+$. Another event, by far our most spectacular one, can be interpreted as having a muon, a charged pion, and two gamma rays presumably from a neutral pion. Over 2 BeV of energy release is seen in the chamber. This could in principle be an example of $w^+ \rightarrow \pi^+ + \pi^0$. Finally, we have one event, Fig. 6(A), in which both a muon and an electron appear to leave the same vertex. If this were a boson production, it would correspond to the boson decay mode $w^+ \rightarrow e^+ + \nu$. The alternative explanation for this event would require (i) that a neutral pion be produced with the muon; and (ii) that one of its gamma rays convert in the plate of the interaction while the other not convert visibly in the chamber.

The difficulty of demonstrating the existence of a boson is inherent in the poor resolution of the chamber. Future experiments should shed more light on this interesting question.

Neutrino cross sections. We have attempted to compare our observations with the predicted

cross sections for reactions (2) using the theory.¹⁻³ To include the fact that the nucleons in (2) are, in fact, part of an aluminum nucleus, a Monte Carlo calculation was performed using a simple Fermi model for the nucleus in order to evaluate the effect of the Pauli principle and nucleon motion. This was then used to predict the number of "elastic" neutrino events to be expected under our conditions. The results agree with simpler calculations based on Fig. 2 to give, in terms of number of circulating protons,

from $\pi \rightarrow \mu + \nu$,	0.60 events/ 10^{16} protons,
from $K \rightarrow \mu + \nu$,	0.15 events/ 10^{16} protons,
Total	0.75 events/ $10^{16} \pm \sim 30\%$.

The observed rates, assuming all single muons are "elastic" and all vertex events "inelastic" (i.e., produced with pions) are

"Elastic":	0.84 ± 0.16 events/ 10^{16} (29 events),
"Inelastic":	0.63 ± 0.14 events/ 10^{16} (22 events).

The agreement of our elastic yield with theory indicates that no large modification to the Fermi interaction is required at our mean momentum transfer of 350 MeV/c. The inelastic cross section in this region is of the same order as the elastic cross section.

Neutrino flip hypothesis. Feinberg, Gursev, and Pais¹⁷ have pointed out that if there were two different types of neutrinos, their assignment to muon and electron, respectively, could in principle be interchanged for strangeness-violating weak interactions. Thus it might be possible that

$$\begin{array}{ccc} \pi^+ \rightarrow \mu^+ + \nu_1 & \text{while} & K^+ \rightarrow \mu^+ + \nu_2 \\ \pi^+ \rightarrow e^+ + \nu_2 & & K^+ \rightarrow e^+ + \nu_1. \end{array}$$

This hypothesis is subject to experimental check by observing whether neutrinos from $K_{\mu 2}$ decay produce muons or electrons in our chamber. Our calculation of the neutrino flux from $K_{\mu 2}$ decay indicates that we should have observed 5 events from these neutrinos. They would have an average energy of 1.5 BeV. An electron of this energy would have been clearly recognizable. None have been seen. It seems unlikely therefore that the neutrino flip hypothesis is correct.

The authors are indebted to Professor G. Feinberg, Professor T. D. Lee, and Professor C. N. Yang for many fruitful discussions. In particular, we note here that the emphasis by Lee and Yang on the importance of the high-energy behavior of

weak interactions and the likelihood of the existence of two neutrinos played an important part in stimulating this research.

We would like to thank Mr. Warner Hayes for technical assistance throughout the experiment. In the construction of the spark chamber, R. Hodor and R. Lundgren of BNL, and Joseph Shill and Yin Au of Nevis did the engineering. The construction of the electronics was largely the work of the Instrumentation Division of BNL under W. Higinbotham. Other technical assistance was rendered by M. Katz and D. Balzarini. Robert Erlich was responsible for the machine calculations of neutrino rates, M. Tannenbaum assisted in the Cosmotron runs.

The experiment could not have succeeded without the tremendous efforts of the Brookhaven Accelerator Division. We owe much to the cooperation of Dr. K. Green, Dr. E. Courant, Dr. J. Blewett, Dr. M. H. Blewett, and the AGS staff including J. Spiro, W. Walker, D. Sisson, and L. Chimienti. The Cosmotron Department is acknowledged for its help in the initial assembly and later calibration runs.

The work was generously supported by the U. S. Atomic Energy Commission. The work at Nevis was considerably facilitated by Dr. W. F. Goodell, Jr., and the Nevis Cyclotron staff under Office of Naval Research support.

*This research was supported by the U. S. Atomic Energy Commission.

†Alfred P. Sloan Research Fellow.

¹T. D. Lee and C. N. Yang, Phys. Rev. Letters 4, 307 (1960).

²Y. Yamaguchi, Progr. Theoret. Phys. (Kyoto) 6, 1117 (1960).

³N. Cabibbo and R. Gatto, Nuovo cimento 15, 304 (1960).

⁴G. Feinberg, Phys. Rev. 110, 1482 (1958).

⁵Several authors have discussed this possibility. Some of the earlier viewpoints are given by: E. Konopinski and H. Mahmoud, Phys. Rev. 92, 1045 (1953); J. Schwinger, Ann. Phys. (New York) 2, 407 (1957); I. Kawakami, Progr. Theoret. Phys. (Kyoto) 19, 459 (1957); M. Konuma, Nuclear Phys. 5, 504 (1958); S. A. Bludman, Bull. Am. Phys. Soc. 4, 80 (1959); S. Oneda and J. C. Pati, Phys. Rev. Letters 2, 125 (1959); K. Nishijima, Phys. Rev. 108, 907 (1957).

⁶T. D. Lee and C. N. Yang (private communications). See also Proceedings of the 1960 Annual International Conference on High-Energy Physics at Rochester (Interscience Publishers, Inc., New York, 1960), p. 567.

⁷D. Bartlett, S. Devons, and A. Sachs, Phys. Rev. Letters 8, 120 (1962); S. Frankel, J. Halpern, L. Holloway, W. Wales, M. Yearian, O. Chamberlain, A. Lemonick, and F. M. Pipkin, Phys. Rev. Letters 8, 123 (1962).

⁸B. Pontecorvo, J. Exptl. Theoret. Phys. (U.S.S.R.) 37, 1751 (1959) [translation: Soviet Phys. - JETP 10, 1236 (1960)].

⁹M. Schwartz, Phys. Rev. Letters 4, 306 (1960).

¹⁰W. F. Baker et al., Phys. Rev. Letters 7, 101 (1961).

¹¹R. L. Cool, L. Lederman, L. Marshall, A. C. Melissinos, M. Tannenbaum, J. H. Tinlot, and T. Yamanouchi, Brookhaven National Laboratory Internal Report UP-18 (unpublished).

¹²These will be published in a more complete report.

¹³H. L. Anderson, T. Fujii, R. H. Miller, and L. Tau, Phys. Rev. 119, 2050 (1960); G. Culligan, J. F. Lathrop, V. L. Telegdi, R. Winston, and R. A. Lundy, Phys. Rev. Letters 7, 458 (1961); R. Hildebrand, Phys. Rev. Letters 8, 34 (1962); E. Bleser, L. Lederman, J. Rosen, J. Rothberg, and E. Zavattini, Phys. Rev. Letters 8, 288 (1962).

¹⁴R. Feynman and M. Gell-Mann, Phys. Rev. 109, 193 (1958); R. Marshak and E. Sudershan, Phys. Rev. 109, 1860 (1958).

¹⁵R. Plano, Phys. Rev. 119, 1400 (1960).

¹⁶T. D. Lee, P. Markstein, and C. N. Yang, Phys. Rev. Letters 7, 429 (1961).

¹⁷G. Feinberg, F. Gurse, and A. Pais, Phys. Rev. Letters 7, 208 (1961).

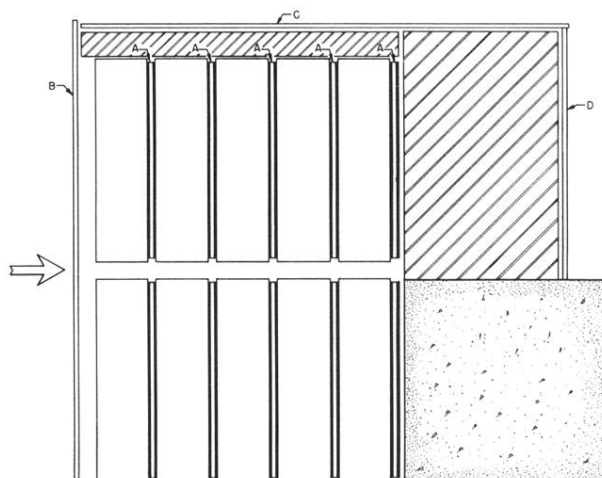


FIG. 3. Spark chamber and counter arrangement. *A* are the triggering slabs; *B*, *C*, and *D* are anticoincidence slabs. This is the front view seen by the four-camera stereo system.

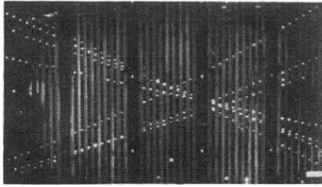


FIG. 4. Land print of Cosmic-ray muons integrated over many incoming tracks.

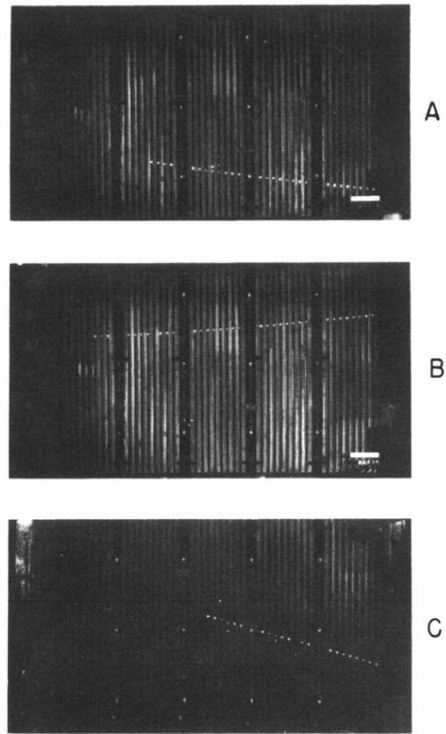


FIG. 5. Single muon events. (A) $p_\mu > 540$ MeV and δ ray indicating direction of motion (neutrino beam incident from left); (B) $p_\mu > 700$ MeV/c; (C) $p_\mu > 440$ with δ ray.

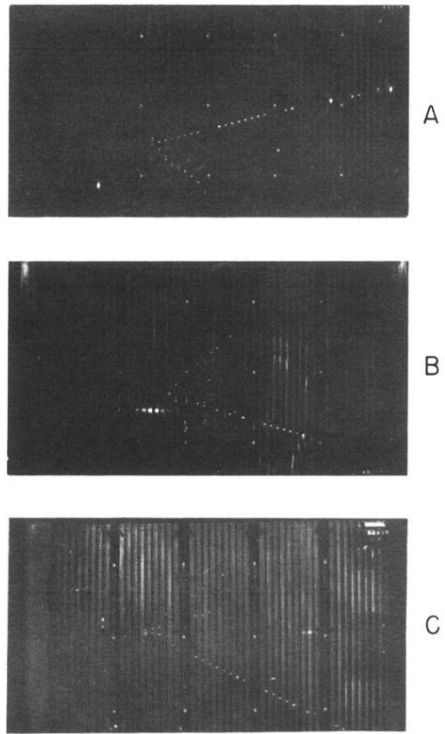


FIG. 6. Vertex events. (A) Single muon of $p_{\mu} > 500$ MeV and electron-type track; (B) possible example of two muons, both leave chamber; (C) four prong star with one long track of $p_{\mu} > 600$ MeV/c.

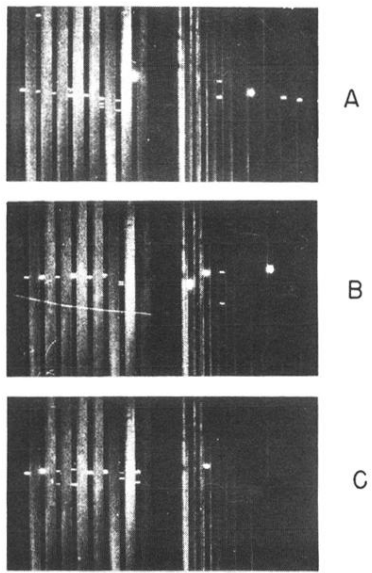


FIG. 8. 400-MeV electrons from the Cosmotron.